RSC Advances

PAPER

View Article Online
View Journal | View Issue

Cite this: *RSC Adv.*, 2023, **13**, 2225

An ionic Fe-based metal–organic-framework with 4′-pyridyl-2,2′:6′,2″-terpyridine for catalytic hydroboration of alkynes†

Guoqi Zhang, *[a] Shengping Zheng [b] and Michelle C. Neary [b]

An ionic metal–organic-framework (MOF) containing nanoscale channels was readily assembled from ditopic 4′-pyridyl-2,2′:6′,2″-terpyridine (pytpy) and a simple iron(II) salt. X-ray structural analysis revealed a two-dimensional grid-like framework assembled by classic octahedral $(pytpy)_2Fe^{II}$ cations as linkers (with pytpy as a new ditopic pyridyl ligand) and octa-coordinate $FeCl_2$ centers as nodes. The layer-by-layer assembly of the 2-D framework resulted in the formation of 3-D porous materials consisting of nano-scale channels. The charges of the cationic framework were balanced with anionic $Cl_3FeOFeCl_3$ in its void channels. The new Fe-based MOF material was employed as a precatalyst for *syn*-selective hydroboration of alkynes under mild, solvent-free conditions in the presence of an activator, leading to the synthesis of a range of *trans*-alkenylboronates in good yields. The larger scale applicability and recyclability of the new MOF catalyst was further explored. This represents a rare example of an ionic MOF material that can be utilized in hydroboration catalysis.

Received 17th December 2022
Accepted 5th January 2023

DOI: 10.1039/d2ra08040k

rsc.li/rsc-advances

Introduction

Hydroboration of unsaturated hydrocarbons provides a facile and direct approach to organoborane compounds that have been used as crucial organic synthons in numerous carbon–carbon bond forming processes. For example, the hydroboration of alkynes with pinacolborane (HBpin) or catecholborane (HBcat) leads to formation of alkenylboronate esters which can serve as key precursors in the classic Miyaura–Suzuki coupling reaction and other organic transformations.[1,2] The first catalytic hydroboration, of 3-hexyne with HBcat, was developed by Männig and Nöth in 1985 using Rh.[3] A number of noble metal catalysts (such as Pd, Pt, Ru, Rh, Ir, Au and Ag) have been explored since then,[4] but efforts in recent years have resulted in a surge of effective earth-abundant metal catalysts with various organic ligands.[5] A catalyst-free version has also been recently reported, however, elevated temperature was required to initiate reactivity (100 °C in toluene).[6]

Iron, as the most earth-abundant transition metal, is particularly attractive in replacing precious metals for key catalytic conversions such as hydrogenation and hydrofunctionalizations.[7] Molecular Fe-based catalysts thus have long been a research focus, taking advantage of their low cost, low toxicity and environmental sustainability.[8] Several well-defined iron catalysts for the hydroboration of alkynes have been developed in the past decade, as summarized in Scheme 1. Both *syn*- and *anti*-selective hydroboration of terminal alkynes by distinct iron catalysts has been established, with *syn*-hydroboration process being the majority (Scheme 1).[9–16] In 2013, the Thomas group reported an iron complex of bis(imino)pyridine that, upon activation with EtMgBr, displayed good *syn*-selective catalytic activity towards a range of alkenes, where two examples of internal alkynes were included.[9] A few years later, Nishibayashi and coworkers developed a pincer-PNP iron hydride catalyst for effective *syn*-selective hydroboration of a range of terminal alkynes without the presence of an activator, though inferior activity was found for internal alkynes.[10] Recently, Findlater's group deployed a Fe(I) catalyst of bis(arylimino)-acenaphthene ligands that promoted alkyne hydroboration with good stereo- and regioselectivity in the presence of activators (NaO^tBu or $NaHBEt_3$) at 70 °C.[11] In the same year, it was reported that the structurally defined Fe–H complex, $FeH(CO)(NO)(Ph_3P)_2$, enables stereoselective hydroboration of a variety of internal alkynes at 80 °C using either HBpin or bis(pinacolato)diboron (B_2pin_2) as a boron source.[12] In addition, Fe-catalysed *syn*-selective hydroboration has been also carried out using simple $Fe_2(CO)_9$ (ref. 13) and Fe_3O_4 (ref. 14) nanoparticles as precatalysts. In contrast, *anti*-selective alkyne hydroboration has rarely been achieved by Fe catalysts. Examples include two well-defined Fe–H complexes of PNP and PCP

[a]*Department of Sciences, John Jay College, PhD Program in Chemistry, The Graduate Center, The City University of New York, New York, NY 10019, USA. E-mail: guzhang@jjay.cuny.edu*

[b]*Department of Chemistry, Hunter College, The City University of New York, New York, 10065 NY, USA*

† Electronic supplementary information (ESI) available. CCDC 2175907 and 2175908. For ESI and crystallographic data in CIF or other electronic format see DOI: https://doi.org/10.1039/d2ra08040k

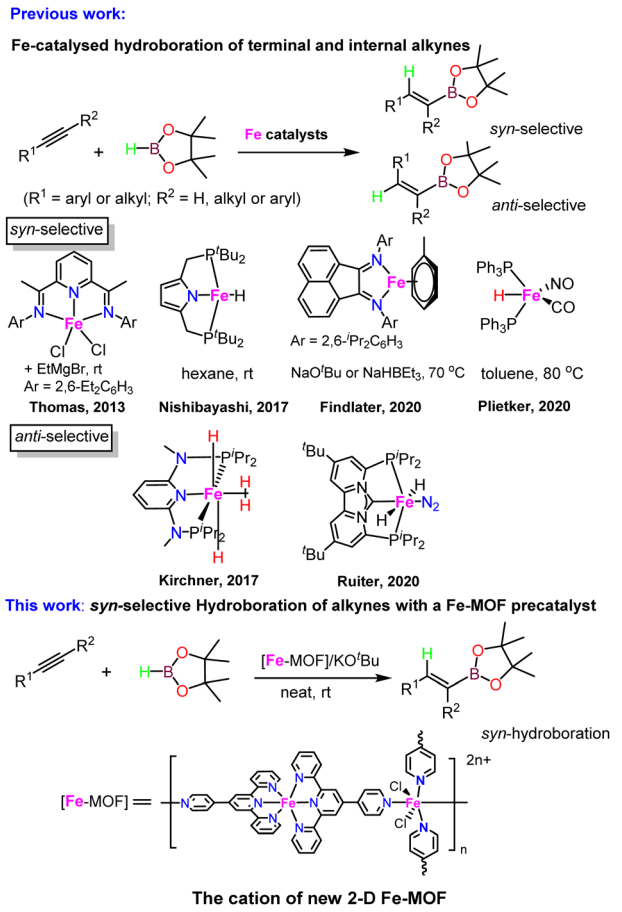

Scheme 1 The state-of-the-art of iron-catalysed hydroboration of alkynes and the results presented in this work.

pincer ligands, reported by the Kirchner and Ruiter groups, respectively.[15,16]

We have recently developed a handful of hydroboration catalysts of V, Mn and Al using a common tridentate chelating ligand, 2,2′:6′,2″-terpyridine (tpy, Scheme 2).[17] The redox-noninnocent nature of tpy was found to be critical in the formation of vanadium(III) and aluminum(III) complexes as well as in the catalytic cycles. We have further explored the expanded ditopic ligand **L1** towards the synthesis of one-dimensional coordination polymers of cobalt and manganese, and their use as precatalysts in extremely high-efficiency hydroboration of unsaturated bonds.[18] While iron has been frequently employed for tpy coordination chemistry, catalytically active Fe–tpy coordination frameworks have been sparsely reported,[19] due to the formation of a stable octahedral geometry around Fe(II) with homoleptic tpy ligands.[20] In search of well-defined polymeric catalysts of iron with tpy-type ligands, we report here our observation of a rare bench-stable 3-D Fe-MOF assembled from the direct reaction of ligand **L1** with $FeCl_2$, and its ability to act as a precatalyst for the *syn*-selective hydroboration of alkynes. This represents the first example of an ionic Fe-based MOF material as a catalyst for selective alkyne hydroboration under mild conditions.

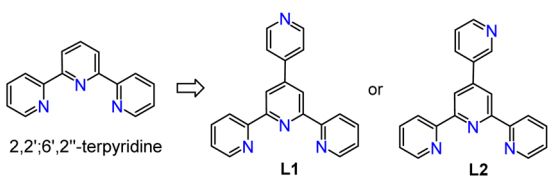

Scheme 2 The structures of tpy derivatives used as ligands in this work.

Results and discussion

Carefully layering a CH_2Cl_2–MeOH solution of **L1** with a MeOH solution of 2.0 equiv. of $FeCl_2 \cdot 4H_2O$ gave rise to the formation of dark-brown crystalline blocks of **1** in 74% yield after two weeks. **1** was characterized by IR, elemental analysis and single-crystal X-ray diffraction. X-ray diffraction analysis confirmed that **1** crystallizes in the monoclinic $P2_1/n$ space group. An ORTEP representation of the repeating structural unit showing the coordination environments of the three independent Fe^{II} centers is drawn in Fig. 1. As expected, homoleptic octahedral Fe^{II} centers were formed *via* two tridentate tpy chelators, which serve as linear bridging bis(pyridyl) ligands. Four of these molecules are bound to another Fe^{II} center as monodentate ligands, with two chloride ligands sitting at the axial direction. Two counterions of $Cl_3FeOFeCl_3$ (ref. 21) co-crystallised in each asymmetric unit to balance the charges of the homoleptic Fe^{II} centers. The Fe–N bond lengths of the homoleptic Fe^{II} centers (Fe1 and Fe3) are between 1.869(10) and 1.998(10) Å, while those

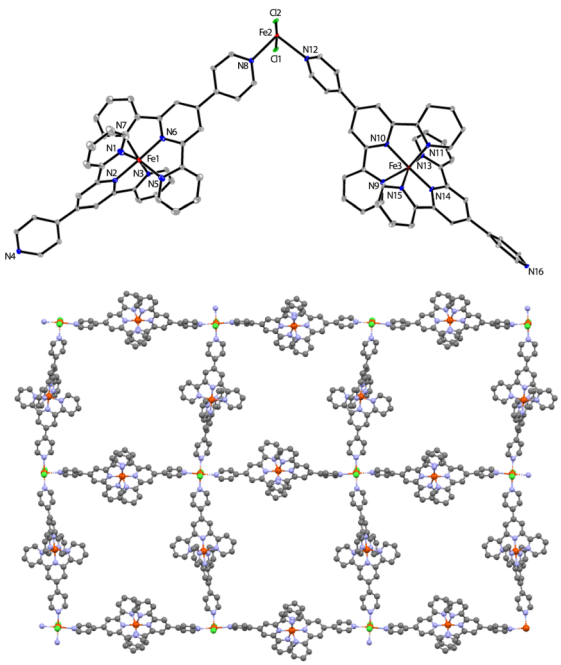

Fig. 1 The ORTEP diagram of the independent molecular cation of **1** (top) with thermal ellipsoids drawn at the 30% probability level, and a ball-and-stick representation of the 2-D grid-like framework (bottom). H atoms, counterions $Cl_3FeOFeCl_3$ and co-crystallised solvent molecules are omitted for clarity.

around the FeN_4Cl_2 center (Fe2) are significantly longer (in the range of 2.226(9)–2.320(9) Å). The latter Fe2 center with two axial chloride ligands could serve as an active reactive site through ligand exchange during catalysis. Expansion of the connectivity leads to the observation of a uniform 2-D grid-like framework, as displayed in Fig. 1. The large, nanoscale grid in the framework adopts a dimension of 2.2 × 2.2 nm, with diagonal Fe···Fe distances of ~3.0–3.3 nm. The layer-by-layer packing of the 2-D framework is driven mainly by π···π stacking to form a 3-D MOF in which large void channels are present (see Fig. S5 in the ESI†). A number of cocrystallized solvent molecules (MeOH and H_2O) are found in the void space in the X-ray structure, but they could be readily removed upon exposure to air for several hours, as evidenced by the microanalytic data of an air-dried sample. It is worth mentioning that ionic MOF materials such as these are appealing in multifunctional applications and usually challenging to synthesize,[22] and Fe-based ionic MOFs are extremely rare.[23] The powder X-ray diffraction analysis of a bulk sample of **1** shows a relatively poor diffraction pattern despite several attempts using different diffractors, indicating that the material may partially lose its crystallinity upon the removal of solvated molecules from the porous framework. In addition, X-ray photoelectron spectroscopy (XPS) analysis reveals the presence of both Fe^{2+} and Fe^{3+} in **1**, consistent with the X-ray crystallographic results. The porosity of **1** was determined by BET surface area analysis and a relatively small BET surface area of 3.86 $m^2\ g^{-1}$ was detected (see ESI†).

In an attempt to synthesize a similar Fe-MOF structure, the closely related ligand **L2** was instead employed using the same procedure. However, a discrete, mononuclear homoleptic Fe^{II} complex (**2**) was obtained, in which one of the uncoordinated pyridyl-N atoms is protonated (Fig. 2). Again, counterions Cl_3-$FeOFeCl_3$ (1.5 per octahedral Fe^{II} center) were found to balance the protonated cationic complex in the unit cell.

With new Fe materials in hand, catalytic reactions for the hydroboration of alkynes were then investigated. We chose phenylacetylene as a model substrate and HBpin as a boron source, and the results are summarized in Table 1. The initial test was carried out using **1** (0.2 mol%) and potassium *tert*-butoxide (KO^tBu) as an activator in tetrahydrofuran at room temperature. It was pleasing to notice that the *syn*-alkenylboronate product β-(*E*)-**3a** was detected in moderate 65% yield by gas chromatography (GC) analysis, along with a small amount

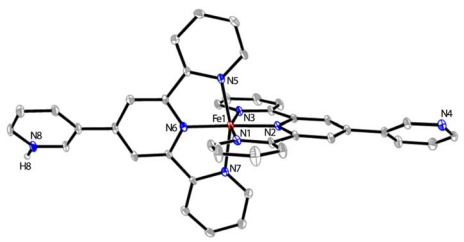

Fig. 2 The ORTEP diagram of the independent molecular cation of **2** with thermal ellipsoids drawn at the 30% probability level. H atoms bound to carbons are omitted for clarity.

Table 1 Condition screening for hydroboration of phenylacetylene with HBpin[a]

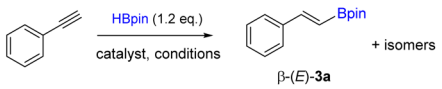

β-(*E*)-**3a**

Entry	Catalyst	Additive	Solvent	Yield of β-(*E*)-**3a**[b] (%)
1	**1**	KO^tBu	THF	65
2	**2**	KO^tBu	THF	5
3	**1**	None	THF	<5
4	None	KO^tBu	THF	<5
5	**1**	NaO^tBu	THF	52
6	**1**	LiO^tBu	THF	46
7	**1**	KOMe	THF	30
8	**1**	K_2CO_3	THF	<5
9	**1**	$LiNTf_2$	THF	<5
10	**1**	$NaHBEt_3$	THF	42
11	**1**	$KHBEt_3$	THF	50
12	**1**	KO^tBu	Toluene	<5
13	**1**	KO^tBu	Et_2O	<5
14[c]	**1**	KO^tBu	DMSO	78
15	**1**	KO^tBu	Neat	82
16[d]	**1**	KO^tBu	Neat	83
17[e]	**1**	KO^tBu	Neat	Trace

[a] Conditions: phenylacetylene (0.5 mmol), pinacolborane (0.6 mmol), **1** (0.2 mol% based on $Fe_3(L)_4$ unit), additive (1 mol%) and solvent (0.5 mL), rt, N_2, 16 h. Other isomeric products were detected with <5% yield unless otherwise stated. [b] Determined by GC analysis with hexamethylbenzene as an internal standard. [c] Regioisomer α-**3a** was detected in 8% yield. [d] 1 mol% of **1** was used. [e] Reaction run in the air. $LiNTf_2$: lithium bis(trifluoromethane)sulfonimidate.

(<5%) of other isomeric products (entry 1, Table 1). In contrast, when **2** was used for the reaction under the same conditions, only 5% of the desired product was detected (entry 2). The inactivity of **2** as a catalyst here is consistent with the fact that in **2**, Fe^{II} is in an saturated octahedral geometry with homoleptic ligands. Control experiments were conducted to examine the importance of **1** and an additive (entries 3 and 4). It was found that both **1** and the additive were required to achieve good reactivity. Next, we explored the influence of various base additives on the catalytic activity. From the results using 7 different additives, we found KO^tBu was the best (entries 5–11). Finally, solvent effect was investigated to seek the best media for this reaction (entries 12–14). It was found that the reaction proceeded more smoothly in DMSO than in THF, while toluene and diethyl ether were not suitable solvents. It was further observed that the reaction actually performed better without a solvent (entry 15), where 82% yield of β-(*E*)-**3a** was detected. An attempt to improve the yield by increasing the amount of **1** to 1 mol% proved unsuccessful (entry 16). It was also noted that the reaction did not proceed at all in the air (entry 17).

In the next step, we employed the optimal reaction conditions obtained above (entry 15, Table 1) to a variety of alkynes. The results are summarized in Scheme 3. Substituted phenylacetylenes bearing methyl, fluoro or methoxy groups are suitable substrates for the hydroboration using **1** as a precatalyst, affording the corresponding alkenylboronate products **3b–d** with

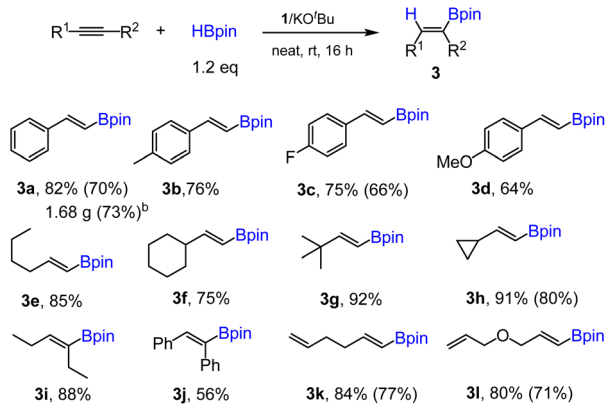

Scheme 3 **1**-Catalysed *syn*-hydroboration of various alkynes.[a] [a]Conditions: **1** (0.2 mol%), aldehyde (1.0 mmol) and HBpin (1.1 mmol), neat, 25 °C, 16 h, N_2. GC yields are determined using hexamethylbenzene as an internal standard. Yields of isolated products are given in parenthesis. [b]Reaction run at a 10 mmol scale.

good yields. Aliphatic terminal alkynes are also well hydroborated under the standard conditions to give aliphatic boronate products **3e–h** with high yields. The hydroboration of aliphatic internal alkynes was demonstrated by using 3-hexyne and *trans*-stilbene for the synthesis of **3i** and **3j**, respectively. Finally, two substrates containing both terminal alkene and alkyne groups were examined, and excellent chemoselectivity towards alkyne over alkene was observed, with both products **3k** and **3l** being isolated in appreciable yields. Unfortunately, alkynes containing heterocyclic groups such as 4-ethynylpyridine and 3-ethynylthiophene were not suitable substrates for this reaction. To demonstrate the applicability of this method, a gram-scale reaction was performed using phenylacetylene as the substrate. Thus, **3a** (1.68 g) was readily isolated in 73% yield while using 10 mmol of starting materials (Scheme 3).

To further exploit the ability of the **1**/KO^{t}Bu system for the hydroboration of other common unsaturated bonds, we applied the standard catalytic conditions to acetophenone and styrene (Scheme 4). It was found that ketone could be readily hydroborated quantitively in one hour, while the hydroboration of styrene was regioselective, giving the branched and linear alkylboronate products (b/l = 10 : 1) in good total yield. Such regioselectivity has been previously reported using a structurally related 1-D Co(II) coordination polymer of **L1**.[18b] Finally, intermolecular competing experiments were carried out to further demonstrate chemoselective hydroboration. Thus, the hydroboration of phenylacetylene was conducted in the presence of equimolar acetophenone or styrene, respectively (Scheme 4). The results revealed that the ketone was selectively converted to the alkylboronate ester, while the alkyne remained intact. Phenylacetylene was the preferred substrate over styrene, in agreement with the results from the intramolecular competing hydroboration as seen in Scheme 3.

Since the catalytic reactions by **1** were heterogeneous, as the dark-brown solid could be fully recovered after the reaction by simply decanting the liquid and washing with THF (Fig. 3), we have performed recycling and reusing experiments to demonstrate its recyclability. Thus, **1** recovered from the standard hydroboration of phenylacetylene was reused for the next run by reloading the additive (1 mol%) and reactants, and the yield of product **3a** was found to remain almost unchanged (80% *vs.* 82%). Meanwhile, the leaching of Fe from the MOF during the 1st run was found to be negligible as analysed by inductively coupled plasma optical emission spectrometry (ICP-OES). The same procedure was then applied to four more runs with recycled MOF catalyst, and the yield of **3a** remained at the same level (ESI†). This indicates the ability of **1** as a facile and effective recyclable precatalyst for practical applications. The PXRD of a recycled sample of **1** reveals a similar, poor diffraction pattern to the one prior to catalytic reaction. The XPS analysis of fresh and recycled samples of **1** reveals identical oxidation states and binding modes of all elements. Interestingly, the BET surface area (13.04 $m^2\ g^{-1}$) of recycled material of **1** is much higher than the unused sample, indicating a possible phase change during the catalytic conversion.

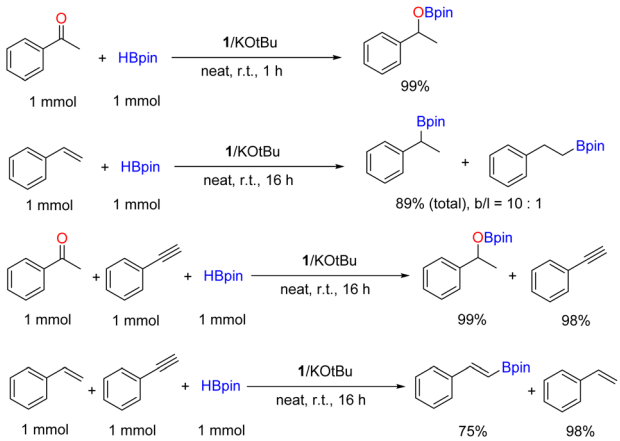

Scheme 4 Hydroboration of ketone and styrene as well as chemoselective hydroboration catalysed by **1**/KO^{t}Bu under standard conditions. Yields (and b/l ratio) were determined by GC analysis using hexamethylbenzene as an internal standard.

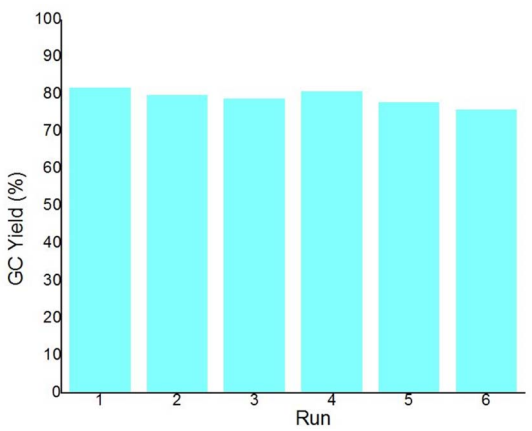

Fig. 3 The bar graph results of recycling experiments for **1**-catalysed hydroboration of phenylacetylene.

Experimental

General considerations

Unless specified otherwise, all reactions were carried out under a dry nitrogen atmosphere using standard glovebox and Schlenk techniques. Deuterated solvents were purchased from Cambridge Isotope Laboratories. Anhydrous grade solvents (stored over 4 Å molecular sieves) and alkyne substrates were purchased from Sigma-Aldrich, Fisher Scientific and TCI America. Pinacolborane was purchased from Alfa Aesar and used as received. FT-IR spectra were recorded on a Shimadzu 8400S instrument with solid samples under N_2 using a Golden Gate ATR accessory. ^{1}H NMR and ^{13}C NMR spectra were obtained at room temperature on a Bruker AV 500 or 600 MHz NMR spectrometer, with chemical shifts (δ) referenced to the residual solvent signal. Inductively coupled plasma optical emission spectrometry (ICP-OES) analyses were conducted by Robertson Microlit Laboratories in the US. X-ray powder diffraction was conducted on a PANalytical X'Pert Pro Powder Diffractometer using a PIXcel^{1D} detector at City College of New York. XPS analysis was conducted by MSE Supplies LLC in the US using Thermo Scientific ESCALAB 250Xi and Kratos AXIS-ULTRA DLD-600 W instruments. Measurement of BET surface area was performed by MSE Supplies LLC in the US using Quantachrome SI or Micromeritics ASAP 2460 facilities. GC-MS analysis was obtained using a Shimadzu GCMS-QP2010S gas chromatograph mass spectrometer. Elemental analyses were performed by Midwest Microlab LLC in Indianapolis in the US. **L1** and **L2** were prepared according to the literature.[24]

Synthesis of 1

A solution of ligand **L1** (31.0 mg, 0.100 mmol) in MeOH/CH_2Cl_2 (10 mL, 1 : 3, v/v) was placed in a test tube. A blank solution of MeOH/CH_2Cl_2 (4 mL, 1 : 1, v/v) was layered on the top of the ligand solution, followed by a solution of $FeCl_2 \cdot 4H_2O$ (39.6 mg, 0.200 mmol) in MeOH (8 mL). The tube was sealed and allowed to stand at room temperature for about 2 weeks, during which time X-ray quality dark brown block-like crystals grew at the wall and bottom of the tube. The crystals were collected by decanting the solvent, washing with MeOH and then drying *in vacuo*. Yield: 40.0 mg (74% based on **L1**). FT-IR (solid, cm^{-1}): 3389 br, 3062 w, 1600 s, 1481 w, 1410 s, 1361 m, 1286 m, 1246 w, 1158 m, 1028 s, 824 s, 786 s, 751 s, 732 m. Anal. calcd. for $C_{80}H_{56}Cl_{14}Fe_7N_{16}O_2$: C 44.47, H 2.61, N 10.37. Found C 45.05, H 2.86, N 10.45%. The co-crystallised solvents (MeOH and H_2O) did not remain in the MOF for the elemental analysis.

Synthesis of 2

A solution of ligand **L2** (31.0 mg, 0.100 mmol) in MeOH/PhCl (10 mL, 1 : 3, v/v) was placed in a test tube. A blank solution of MeOH/PhCl (4 mL, 1 : 1, v/v) was layered on the top of the ligand solution, followed by a solution of $FeCl_2 \cdot 4H_2O$ (39.6 mg, 0.200 mmol) in MeOH (8 mL). The tube was sealed and allowed to stand at room temperature for about 2 weeks, during which time X-ray quality brown plate-like crystals grew at the wall and bottom of the tube. The crystals were collected by decanting the solvent, washing with MeOH, and then drying *in vacuo*. Yield: 40.2 mg (65%). FT-IR (solid, cm^{-1}) 3070 m, 1603 m, 1538 m, 1464 m, 1402 s, 1246 s, 1054 s, 1025 s, 843 s, 784 s, 749 s, 627 m. Anal. calcd. for $C_{43}H_{31.5}Cl_{9.5}Fe_4N_8O_{1.5}$: C 41.50, H 2.55, N 9.00. Found C 41.86, H 2.79, N 9.22%.

General procedure for catalytic hydroboration of alkynes

In a glovebox under N_2 atmosphere, **1** (4.3 mg, 0.2 mol%) and potassium *tert*-butoxide (1.1 mg, 1 mol%) were placed in a 3.8 mL glass vial equipped with a stir bar, to which alkynes (1.0 mmol) and pinacolborane (1.2 mmol, 1.2 equiv.) were then added. The reaction mixture was allowed to stir at room temperature for 16 h. The reaction was exposed to the air and the crude reaction mixture was analyzed by GC-MS using hexamethylbenzene as an internal standard and then purified through column chromatography (SiO_2) using ethyl acetate/hexane as an eluent. Selective alkenylboronate products were characterized by ^{1}H and ^{13}C NMR spectroscopies.

Gram-scale experiment

In a glovebox under N_2 atmosphere, **1** (43 mg, 0.2 mol%) and potassium *tert*-butoxide (11 mg, 1 mol%) were placed in a 20 mL disposal vial equipped with a stir bar, to which phenylacetylene (1.02 g, 10 mmol) and pinacolborane (1.55 g, 12 mmol, 1.2 equiv.) were then added. The reaction mixture was allowed to stir at room temperature for 16 h. The crude product was subject to a flash column chromatography (silica gel) using ethyl acetate/hexane (1 : 10, v/v) as an eluent. **3a** was isolated as a colorless oil which was confirmed by ^{1}H and ^{13}C NMR spectroscopies. Yield: 1.68 g (73%).

Procedure for recycling experiments

In a glovebox under N_2 atmosphere, **1** (4.3 mg, 0.2 mol%) and potassium *tert*-butoxide (1.1 mg, 1 mol%) were placed in a 3.8 mL glass vial equipped with a stir bar, to which phenylacetylene (102 mg, 1.0 mmol) and pinacolborane (155 mg, 1.2 mmol, 1.2 equiv.) were then added. The reaction mixture was allowed to stir at room temperature for 16 h. Hexamethylbenzene (5 mg) was added to the mixture which was analyzed by using GC-MS to obtain the yield of **3a**. Then the liquid was carefully removed and the dark brown solid was washed 3 times with THF. The organic extract (1 mL) was combined and analyzed by ICP-OES. The loss of iron from the precatalyst was determined to be 5 ppm, suggesting negligible leaching of Fe from the MOF. The solid that was recovered was then dried under reduced pressure and then placed in a small vial, to which additional KO^{t}Bu (1.1 mg) was added. Then phenylacetylene (102 mg, 1.0 mmol) and pinacolborane (155 mg, 1.2 mmol, 1.2 equiv.) were added. The resultant mixture was stirred at room temperature in air for 16 h and the product was analyzed by using GC analysis again. This procedure was repeated for 4 more cycles and the results of in total 6 runs are summarized in Fig. S1.†

X-ray crystallography

Suitable crystals of **1** and **2** were mounted on cryoloops with Paratone-N oil. X-ray diffraction data were collected on a Bruker

X8 Kappa Apex II diffractometer using Mo Kα radiation. Crystal data, data collection and refinement parameters are summarized in Table S1.† The structures were solved using direct methods and standard difference map techniques, and were refined by full-matrix least-squares procedures on F^2 with SHELXTL (Version 2018/3 for **1** and 2017/1 for **2**).[25] All hydrogen atoms bound to carbon were placed in calculated positions and refined with a riding model [U_{iso}(H) = 1.2–1.5U_{eq}(C)]. For **1**, some hydrogen atoms bound to solvent oxygen atoms were located on the difference map, and others were placed in calculated positions. They were refined with a mixture of distance, angle, and riding restraints [U_{iso}(H) = 1.2U_{eq}(O)]. SQUEEZE/PLATON was used to treat additional solvent molecules as a diffuse contribution to the overall scattering.[26] For **2**, the hydrogen atom bound to nitrogen was located on the difference map and freely refined.

CCDC no. 2175907 and 2175908 contain the supplementary crystallographic data for this paper. Figures for crystal structures were drawn with the programs XP and Mercury v. 2.4. The crystallographic refinement data are listed in Table S1 (ESI).†

Conclusions

In summary, a novel, ionic Fe-MOF structure based on a linear ditopic tpy ligand was readily synthesized and structurally characterized. The 3-D MOF with large void channels has been assembled from a 2-D grid-like cationic network *via* π···π stacking interactions. This represents a rare example of robust Fe-based cationic MOF material. The bench-stable material was used as a precatalyst for the stereo- and regioselective hydroboration of alkynes under mild, solvent-free conditions, and the results were either comparable or superior to other molecular Fe catalysts for this reaction as we documented previously.[9–16] A good substrate scope with functional group tolerance was demonstrated, along with a broader application to ketone and alkene hydroboration. The recyclability of the Fe-MOF precatalyst was demonstrated, highlighting its potential for practical catalytic applications.

Author contributions

G. Z. and S. Z. conceived and supervised the project. G. Z. performed experimental studies. M. C. N. conducted the X-ray crystallographic analysis. All authors analysed the data and wrote the article.

Conflicts of interest

There are no conflicts to declare.

Acknowledgements

We are grateful to the funding support by National Science Foundation for this work (CHE-1900500). We acknowledge the PSC-CUNY awards (63809-0051, 64254-0052 and 65203-0053) from City University of New York and a Seed Grant from the Office for Advancement of Research at John Jay College. Partial support from the American Chemical Society Petroleum Research Fund (#66150-UR1) is also acknowledged.

Notes and references

1 S. Rej, A. Das and T. K. Panda, Overview of Regioselective and Stereoselective Catalytic Hydroboration of Alkynes, *Adv. Synth. Catal.*, 2021, **363**, 4818–4840.

2 (*a*) K. Smith, A. Pelter and H. C. Brown, *Borane Reagent*, Academic Press, London, 1988; (*b*) N. Miyaura and A. Suzuki, Palladium-Catalyzed Cross-Coupling Reactions of Organoboron Compounds, *Chem. Rev.*, 1995, **95**, 2457–2483; (*c*) A. Suzuki, Cross-Coupling Reactions of Organoboranes: An Easy Way to Construct C-C Bonds, *Angew. Chem., Int. Ed.*, 2011, **50**, 6722–6737; (*d*) J. Magano and J. R. Dunetz, Large-Scale Applications of Transition Metal-Catalyzed Couplings for the Synthesis of Pharmaceuticals, *Chem. Rev.*, 2011, **111**, 2177–2250.

3 D. Männig and H. Nöth, Catalytic Hydroboration with Rhodium Complexes, *Angew. Chem., Int. Ed.*, 1985, **24**, 878–879.

4 For representative examples: (*a*) M. Oestreich, E. Hartmann and M. Mewald, Activation of the Si–B Interelement Bond: Mechanism, Catalysis, and Synthesis, *Chem. Rev.*, 2013, **113**, 402–441; (*b*) A. B. Cuenca, R. Shishido, H. Ito and E. Fernández, Transition-metal-free B–B and B–interelement reactions with organic molecules, *Chem. Soc. Rev.*, 2017, **46**, 415–430; (*c*) R. S. Anju, B. Mondal, K. Saha, S. Panja, B. Varghese and S. Ghosh, Chemistry of Diruthenium Analogue of Pentaborane(9) With Heterocumulenes: Toward Novel Trimetallic Cubane-Type Clusters, *Chem.–Eur. J.*, 2015, **21**, 11393–11400; (*d*) C. Gunanathan, M. Holscher, F. F. Pan and W. Leitner, Ruthenium Catalyzed Hydroboration of Terminal Alkynes to *Z*-Vinylboronates, *J. Am. Chem. Soc.*, 2012, **134**, 14349–14352; (*e*) B. Sundararaju and A. Furstner, A *trans*-Selective Hydroboration of Internal Alkynes, *Angew. Chem., Int. Ed.*, 2013, **52**, 14050–14054; (*f*) J. Szyling, A. Franczyk, K. Stefanowska and J. Walkowiak, A recyclable Ru(CO)Cl(H)(PPh_3)$_3$/PEG catalytic system for regio- and stereoselective hydroboration of terminal and internal alkynes, *Adv. Synth. Catal.*, 2018, **360**, 2966–2974; (*g*) A. Leyva, X. Zhang and A. Corma, Chemoselective hydroboration of alkynes vs. alkenes over gold catalysts, *Chem. Commun.*, 2009, 4947–4949; (*h*) T. Ohmura, Y. Yamamoto and N. Miyaura, Rhodium- or Iridium-Catalyzed *trans*-Hydroboration of Terminal Alkynes, Giving (*Z*)-1-Alkenylboron Compounds, *J. Am. Chem. Soc.*, 2000, **122**, 4990–4991; (*i*) Y. Lyu, N. Toriumi and N. Iwasawa, (*Z*)-Selective Hydroboration of Terminal Alkynes Catalyzed by a PSP–Pincer Rhodium Complex, *Org. Lett.*, 2021, **23**, 9262–9266; (*j*) R. Mamidala, V. K. Pandey and A. Rit, $AgSbF_6$-Catalyzed anti-Markovnikov hydroboration of terminal alkynes, *Chem. Commun.*, 2019, **55**, 989–992; (*k*) Q. Feng, H. Wu, X. Li, L. Song, L. W. Chung, Y. D. Wu and J. Sun, Ru-Catalyzed Geminal Hydroboration of Silyl Alkynes via

a New *gem*-Addition Mechanism, *J. Am. Chem. Soc.*, 2020, **142**, 13867–13877.

5 For recent reviews, see: (*a*) J. V. Obligacion and P. J. Chirik, Earth-Abundant Transition Metal Catalysts for Alkene Hydrosilylation and Hydroboration: Opportunities and Assessments, *Nat. Rev. Chem.*, 2018, **2**, 15–34; (*b*) M. D. Greenhalgh, A. S. Jones and S. P. Thomas, Iron-Catalysed Hydrofunctionalisation of Alkenes and Alkynes, *ChemCatChem*, 2015, **7**, 190–222; (*c*) H. Wen, G. Liu and Z. Huang, Recent advances in tridentate iron and cobalt complexes for alkene and alkyne hydrofunctionalizations, *Coord. Chem. Rev.*, 2019, **386**, 138–153; (*d*) S. R. Tamang and M. Findlater, Emergence and Applications of Base Metals (Fe, Co, and Ni) in Hydroboration and Hydrosilylation, *Molecules*, 2021, **24**, 3194.

6 A. K. Jaladi, H. S. Choi and D. K. An, Catalyst-free and solvent-free hydroboration of alkynes, *New J. Chem.*, 2020, **44**, 13626–13632.

7 (*a*) J. Guo, Z. Cheng, J. Chen, X. Chen and Z. Lu, Iron- and Cobalt-Catalyzed Asymmetric Hydrofunctionalization of Alkenes and Alkynes, *Acc. Chem. Res.*, 2021, **54**, 2701–2716; (*b*) M. Y. Hu, P. He, T. Z. Qiao, W. Sun, W. T. Li, J. Lian, J. H. Li and S. F. Zhu, Iron-Catalyzed Regiodivergent Alkyne Hydrosilylation, *J. Am. Chem. Soc.*, 2020, **142**, 16894–16902; (*c*) D. Wei and C. Darcel, Iron-Catalyzed Hydrogen Transfer Reduction of Nitroarenes with Alcohols: Synthesis of Imines and Aza Heterocycles, *J. Org. Chem.*, 2020, **85**, 14298–14306.

8 D. Wei and C. Darcel, Iron Catalysis in Reduction and Hydrometalation Reactions, *Chem. Rev.*, 2018, **119**, 2550–2610.

9 M. D. Greenhalgh and S. P. Thomas, Chemo-, regio-, and stereoselective iron-catalysed hydroboration of alkenes and alkynes, *Chem. Commun.*, 2013, **49**, 11230–11232.

10 K. Nakajima, T. Kato and Y. Nishibayashi, Hydroboration of Alkynes Catalyzed by Pyrrolide-Based PNP Pincer-Iron Complexes, *Org. Lett.*, 2017, **19**, 4323–4326.

11 A. Singh, S. Shafiei-Haghighi, C. R. Smith, D. K. Unruh and M. Findlater, Hydroboration of Alkenes and Alkynes Employing Earth-Abundant Metal Catalysts, *Asian J. Org. Chem.*, 2020, **9**, 416–420.

12 F. Rami, F. Bächtle and B. Plietker, Hydroboration of internal alkynes catalyzed by $FeH(CO)(NO)(PPh_3)_2$: a case of boron-source controlled regioselectivity, *Catal. Sci. Technol.*, 2020, **10**, 1492–1497.

13 M. Haberberger and S. Enthaler, Straightforward Iron-Catalyzed Synthesis of Vinylboronates by the Hydroboration of Alkynes, *Chem.–Asian J.*, 2013, **8**, 50–54.

14 V. S. Rawat and B. Sreedhar, Iron-Catalyzed Borylation Reactions of Alkynes: An Efficient Synthesis of *E*-Vinyl Boronates, *Synlett*, 2014, **25**, 1132–1136.

15 N. Gorgas, L. G. Alves, B. Stöger, A. M. Martins, L. F. Veiros and K. Kirchner, Stable, Yet Highly Reactive Nonclassical Iron(II) Polyhydride Pincer Complexes: *Z*-Selective Dimerization and Hydroboration of Terminal Alkynes, *J. Am. Chem. Soc.*, 2017, **139**, 8130–8133.

16 S. Garhwal, N. Fridman and G. de Ruiter, Z-Selective Alkyne Functionalization Catalyzed by a *trans*-Dihydride N-Heterocyclic Carbene (NHC) Iron Complex, *Inorg. Chem.*, 2020, **59**, 13817–13821.

17 (*a*) G. Zhang, J. Wu, S. Zheng, M. C. Neary, J. Mao, M. Flores, R. J. Trovitch and P. A. Dub, Redox-noninnocent ligand-supported vanadium catalysts for the chemoselective reduction of C=X (X=O, N) functionalities, *J. Am. Chem. Soc.*, 2019, **141**, 15230–15239; (*b*) G. Zhang, H. Zeng, S. Zheng, M. C. Neary and P. A. Dub, Vanadium-Catalyzed Stereo-and Regioselective Hydroboration of Alkynes to Vinyl Boronates, *ACS Catal.*, 2022, **12**, 5425–5429; (*c*) G. Zhang, H. Zeng, J. Wu, Z. Yin, S. Zheng and J. C. Fettinger, Highly Selective Hydroboration of Alkenes, Ketones and Aldehydes Catalyzed by a Well-Defined Manganese Complex, *Angew. Chem., Int. Ed.*, 2016, **55**, 14369–14372; (*d*) G. Zhang, J. Wu, H. Zeng, M. C. Neary, M. Devany, S. Zheng and P. A. Dub, Dearomatization and Functionalization of Terpyridine Ligands Leading to Unprecedented Zwitterionic Meisenheimer Aluminum Complexes and Their Use in Catalytic Hydroboration, *ACS Catal.*, 2019, **9**, 874–884.

18 (*a*) J. Wu, H. S. Zeng, J. Cheng, S. P. Zheng, J. A. Golen, D. R. Manke and G. Zhang, Cobalt (II) coordination polymer as a precatalyst for selective hydroboration of aldehydes, ketones, and imines, *J. Org. Chem.*, 2018, **83**, 9442–9448; (*b*) G. Zhang, J. Wu, S. Li, S. Cass and S. Zheng, Markovnikov-Selective Hydroboration of Vinylarenes Catalyzed by a Cobalt (II) Coordination Polymer, *Org. Lett.*, 2018, **20**, 7893–7897; (*c*) G. Zhang, S. Li, J. Wu, H. Zeng, Z. Mo, K. Davis and S. Zheng, Highly efficient and selective hydroboration of terminal and internal alkynes catalysed by a cobalt (ii) coordination polymer, *Org. Chem. Front.*, 2019, **6**, 3228–3233; (*d*) G. Zhang, H. Zeng, S. Li, J. Johnson, Z. Mo, M. C. Neary and S. Zheng, 1-D manganese(II)-terpyridine coordination polymers as precatalysts for hydrofunctionalisation of carbonyl compounds, *Dalton Trans.*, 2020, **49**, 2610–2615.

19 We reported previously a 2-D Fe-MOF using divergent 4,2′:6′,4″-tpy for hydroboration of carbonyl compounds, see: (*a*) G. Zhang, J. Cheng, K. Davis, M. G. Bonifacio and C. Zajaczkowski, Practical and selective hydroboration of aldehydes and ketones in air catalysed by an iron(II) coordination polymer, *Green Chem.*, 2019, **21**, 1114–1121; (*b*) L. Li, E. Liu, J. Cheng and G. Zhang, Iron (II) coordination polymer catalysed hydroboration of ketones, *Dalton Trans.*, 2018, **47**, 9579–9584.

20 (*a*) J. E. Beves, E. L. Dunphy, E. C. Constable, C. E. Housecroft, C. J. Kepert, M. Newburger, D. J. Price and S. Schaffner, Vectorial property dependence in bis{4′-(n-pyridyl)-2,2′:6′,2″-terpyridine}iron(ii) and ruthenium(ii) complexes with n = 2, 3 and 4, *Dalton Trans.*, 2008, 386–396; (*b*) J. E. Beves, E. C. Constable, S. Decurtins, E. L. Dunphy, C. E. Housecroft, T. D. Keene, M. Neuburger, S. Schaffner and J. A. Zampese, Structural diversity in the reactions of 4′-(pyridyl)-2,2′:6′,2″-terpyridine ligands and bis

{4′-(4-pyridyl)-2,2′:6′,2″-terpyridine}iron(II) with copper(II) salts, *CrystEngComm*, 2009, **11**, 2406–2416.

21 The formation of $Cl_3FeOFeCl_3$ is well-known and has been previously discussed: S. Ameerunisha, J. Schneider, T. Meyer, P. S. Zacharias, E. Bill and G. Henkel, Synthesis and structural characterisation of Fe(II) and Cu(I) complexes of a new tetrafunctional N-donor ligand with dodecahedral or tetrahedral binding domains, *Chem. Commun.*, 2000, 2155–2156.

22 A. Karmakar, A. V. Desai and S. K. Ghosh, Ionic metal-organic frameworks (iMOFs): Design principles and applications, *Coord. Chem. Rev.*, 2016, **307**, 313–341.

23 Q. Hu, J. Yu, M. Liu, A. Liu, Z. Dou and Y. Yang, A Low Cytotoxic Cationic Metal–Organic Framework Carrier for Controllable Drug Release, *J. Med. Chem.*, 2014, **57**, 5679–5685.

24 J. Wang and G. S. Hanan, A Facile Route to Sterically Hindered and Non-Hindered 4′-Aryl-2,2′:6′,2″-Terpyridines, *Synlett*, 2005, **8**, 1251–1254.

25 (*a*) G. M. Sheldrick, *SHELXTL, An Integrated System for Solving, Refining, and Displaying Crystal Structures from Diffraction Data*, University of Göttingen, Göttingen, Federal Republic of Germany, 1981; (*b*) G. M. Sheldrick, SHELXT-Integrated Space-Group and Crystal-Structure Determination, *Acta Crystallogr., Sect. A: Found. Adv.*, 2015, **71**, 3–8.

26 (*a*) A. L. Spek, *PLATON, A Multipurpose Crystallographic Tool*, Utrecht University, Utrecht, The Netherlands, 2005; (*b*) A. L. Spek, Single-crystal structure validation with the program *PLATON*, *J. Appl. Crystallogr.*, 2003, **36**, 7–13.